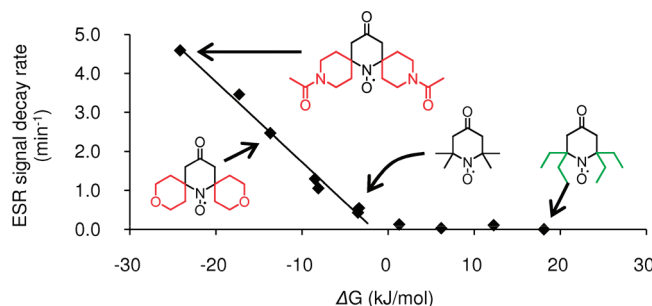


Structure–Reactivity Relationship of Piperidine Nitroxide:  
Electrochemical, ESR and Computational StudiesToshihide Yamasaki,<sup>†</sup> Fumiya Mito,<sup>†</sup> Yuko Ito,<sup>†</sup> Sokkar Pandian,<sup>‡</sup> Yuichi Kinoshita,<sup>†</sup>  
Koji Nakano,<sup>§</sup> Ramachandran Murugesan,<sup>‡,⊥</sup> Kiyoshi Sakai,<sup>||</sup> Hideo Utsumi,<sup>||</sup> and  
Ken-ichi Yamada<sup>\*,†</sup><sup>†</sup>Department of Bio-functional Science, Faculty of Pharmaceutical Sciences, Kyushu University, 3-1-1 Higashi-ku, Maidashi, Fukuoka 812-8582, Japan, <sup>‡</sup>School of Chemistry, Madurai Kamaraj University, Madurai-625021, India, <sup>§</sup>Department of Applied Chemistry, Graduate School of Engineering, Kyushu University, 7-4-4 Moto-oka, Nishi-ku, Fukuoka 819-0395, Japan, <sup>⊥</sup>Networking Resource Center in Biological Sciences, Madurai Kamaraj University, Madurai-625021, India, and <sup>||</sup>Innovation Center for Medical Redox Navigation, Kyushu University, 3-1-1 Higashi-ku, Maidashi, Fukuoka 812-8582, Japan

yamada@pch.phar.kyushu-u.ac.jp

Received October 5, 2010



We have synthesized several nitroxides with different substituents which vary the steric and electronic environment around the N–O moiety and have systematically investigated the role of substituents on the stability of the radicals. Our results demonstrated the reactivity toward ascorbate correlates with the redox potential of the derivatives. Furthermore, ab initio calculations also indicated a correlation between the reduction rate and the computed singly occupied molecular orbital–lowest unoccupied molecular orbital energy gap, but not with solvent accessible surface area of the N–O moiety, supporting the experimental results and suggesting that the electronic factors largely determine the radicals' stability. Hence, it is possible to perform virtual screening of nitroxides to optimize their stability, which can help to rationally design novel nitroxides for their potential use in vivo.

## Introduction

Nitroxides are stable free radicals and are widely used as spin probes,<sup>1–3</sup> antioxidants,<sup>4–6</sup> and radiation protective

agents,<sup>7,8</sup> owing to their interesting redox behavior. The nitroxides are readily oxidized to oxoammonium cations or reduced to hydroxylamines by various in vivo oxidants or reductants.<sup>9</sup> Upon reaction with superoxide, the nitroxides undergo one-electron oxidation and subsequent two-electron reduction, which is driven forward by the redox potential of

\*To whom correspondence should be addressed at Kyushu University. Phone: +81-92-642-6624. Fax: +81-92-642-6626.

(1) Kuppusamy, P.; Li, H.; Ilangovan, G.; Cardounel, A. J.; Zweier, J. L.; Yamada, K.; Krishna, M. C.; Mitchell, J. B. *Cancer Res.* **2002**, *62*, 307.

(2) Matsumoto, K. I.; Hyodo, F.; Matsumoto, A.; Koretsky, A. P.; Sowers, A. L.; Mitchell, J. B.; Krishna, M. C. *Clin. Cancer Res.* **2006**, *12*, 2455.

(3) Yamada, K.; Yamamiya, I.; Utsumi, H. *Free Radical Biol. Med.* **2006**, *40*, 2040.

(4) Wilcox, C. S. *Pharmacol. Ther.* **2010**, *126*, 119.

(5) Utsumi, H.; Yamada, K.; Ichikawa, K.; Sakai, K.; Kinoshita, Y.; Matsumoto, S.; Nagai, M. *Proc. Natl. Acad. Sci. U.S.A.* **2006**, *103*, 1463.

(6) Xavier, S.; Yamada, K.; Samuni, A. M.; Samuni, A.; DeGraff, W.; Krishna, M. C.; Mitchell, J. B. *Biochim. Biophys. Acta* **2002**, *1573*, 109.

(7) Cotrim, A. P.; Hyodo, F.; Matsumoto, K.; Sowers, A. L.; Cook, J. A.; Baum, B. J.; Krishna, M. C.; Mitchell, J. B. *Clin. Cancer Res.* **2007**, *13*, 4928.

(8) Metz, J. M.; Smith, D.; Mick, R.; Lustig, R.; Mitchell, J.; Cherakuri, M.; Glatstein, E.; Hahn, S. M. *Clin. Cancer Res.* **2004**, *10*, 6411.

(9) Kocherginsky, N.; Swartz, H. M. In *Nitroxide Spin Labels: Reactions in Biology and Chemistry*; Kocherginsky, N., Swartz, H. M., Eds.; CRC Press: Boca Raton, FL, 1995; p 27.

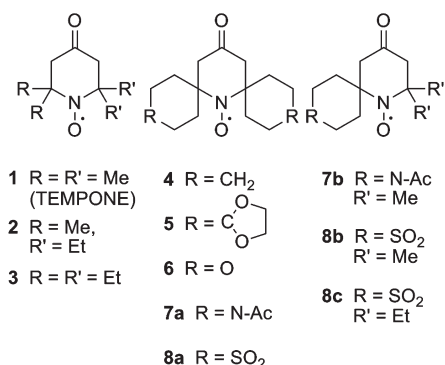
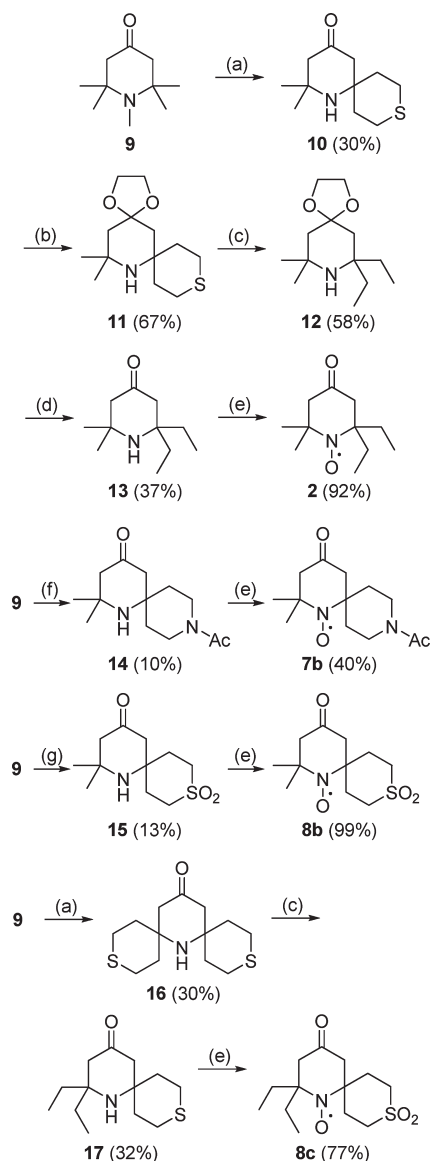


FIGURE 1. Nitroxides used in this study.

the redox couple.<sup>10</sup> The nitroxides are readily reduced by ascorbic acid,<sup>11</sup> posing a limitation to a probe of their in vivo redox status due to their shortened lifetimes. Highly stable nitroxides would be less sensitive to the redox status of their microenvironment. Both the stability and reactivity of nitroxides are equally important for their potential in vivo application. It has been reported that the reduction rate of cyclic nitroxides can be altered by the substituents on the ring.<sup>9,12,13</sup> Recently imidazole and isoindoline nitroxides with ethyl groups proximal to the N–O moiety were reported to be relatively more stable to reduction by ascorbate.<sup>14,15</sup> Although the exact mechanism for this stability is not clearly understood, it could be explained by the steric hindrance the ethyl groups offer the N–O moiety. The electronic environment around the N–O moiety may also influence its stability. A detailed study on the structure–reactivity relationship of the nitroxides is important to understand the underlying mechanism for stability as well as to augment their potential use in vivo.

We previously reported that the 4-oxo-2,2,6,6-tetraethylpiperidine-*N*-oxyl radical showed higher resistance to reduction by ascorbate compared with the methyl substituted analogue,<sup>16</sup> demonstrating the influence of neighboring substituents. Recently, we developed a synthetic strategy to derivatize piperidine-*N*-oxyl radicals at 2 and 6 positions with a wide variety of substituents including spiro rings.<sup>17</sup> Using this method, we have synthesized piperidine-*N*-oxyl derivatives with various steric and electronic environments around the N–O moiety. Herein we report the electrochemical behavior of 2,6-substituted piperidine-*N*-oxyl radicals and their reactivity toward ascorbate. We also report our investigation on the relationship between electrochemical properties and computed structural properties of nitroxides.

## SCHEME 1. Synthetic Scheme of Piperidine Nitroxides<sup>a</sup>



<sup>a</sup>Reagents and conditions: (a) tetrahydro-4*H*-thiopyran-4-one, NH<sub>4</sub>Cl, DMSO; (b) ethylene glycol, PTSA, benzene; (c) Raney-Ni, MeOH; (d) HCl, acetone; (e) H<sub>2</sub>O<sub>2</sub>, Na<sub>2</sub>WO<sub>4</sub>·2H<sub>2</sub>O, MeOH; (f) 1-acetyl-4-piperidone, NH<sub>4</sub>Cl, DMSO; (g) tetrahydro-4*H*-thiopyran-4-one 1,1-dioxide, NH<sub>4</sub>Cl, DMSO.

## Results and Discussion

**Synthesis of Substituted Piperidine-*N*-oxyl Radicals.** Nitroxides used in this study are shown in Figure 1. Nitroxides 3–6, 7a, and 8a were synthesized as previously reported.<sup>17</sup> Nitroxides 2, 7b, 8b, and 8c were synthesized in a similar manner as outlined in Scheme 1. Compound 10 was synthesized from 1,2,2,6,6-pentamethylpiperidin-4-one and tetrahydro-4*H*-thiopyran-4-one. The carbonyl group of 10 was protected with a ketal group and desulfurization was carried out with Raney-Ni<sup>16</sup> to give 12. Subsequent elimination of the ketal group and the oxidation of 13 yielded 2,2-diethyl-6,6-dimethylpiperidin-4-one-*N*-oxyl 2. Compounds 14 and 15 were synthesized with 1-acetyl-4-piperidone and tetrahydro-4*H*-thiopyran-4-one 1,1-dioxide, respectively, as

(10) Krishna, M. C.; Grahame, D. A.; Samuni, A.; Mitchell, J. B.; Russo, A. *Proc. Natl. Acad. Sci. U.S.A.* **1992**, *89*, 5537.

(11) Saphier, O.; Silberstein, T.; Shames, A. I.; Likhtenshtein, G. I.; Maimon, E.; Mankuta, D.; Mazor, M.; Katz, M.; Meyerstein, D.; Meyerstein, N. *Free Radical Res.* **2003**, *37*, 301.

(12) Morris, S.; Sosnovsky, G.; Hui, B.; Huber, C. O.; Rao, N. U.; Swartz, H. M. *J. Pharm. Sci.* **1991**, *80*, 149.

(13) Kirilyuk, I. A.; Bobko, A. A.; Grigor'ev, I. A.; Khramtsov, V. V. *Org. Biomol. Chem.* **2004**, *2*, 1025.

(14) Marx, L.; Chiarelli, R.; Guiberteau, T.; Rassat, A. *J. Chem. Soc., Perkin Trans. 1* **2000**, 1181.

(15) Bobko, A. A.; Kirilyuk, I. A.; Grigor'ev, I. A.; Zweier, J. L.; Khramtsov, V. V. *Free Radical Biol. Med.* **2007**, *42*, 404.

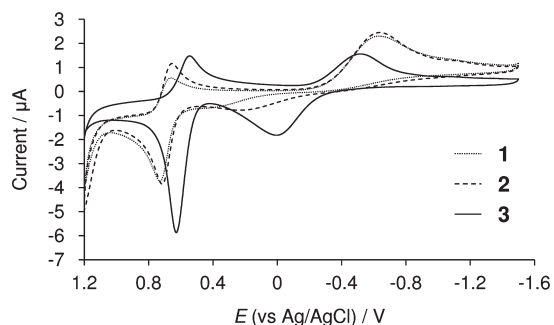
(16) Kinoshita, Y.; Yamada, K.; Yamasaki, T.; Sadasue, H.; Sakai, K.; Utsumi, H. *Free Radical Res.* **2009**, *43*, 565.

(17) Sakai, K.; Yamada, K. i.; Yamasaki, T.; Kinoshita, Y.; Mito, F.; Utsumi, H. *Tetrahedron* **2010**, *66*, 2311.

**TABLE 1.** Experimental Redox Potentials of Oxoammonium Cation/Nitroxide Redox Couple<sup>a</sup>

nitroxide	$E_{pa}^b$	$E_{pc}^c$	$E^{1/2d}$	$\Delta E^e$	$i_{pa}/i_{pc}^f$
<b>1</b>	0.939	0.869	0.904	0.070	2.30
<b>2</b>	0.926	0.860	0.893	0.065	1.56
<b>3</b>	0.806	0.747	0.776	0.058	2.64
<b>4</b>	0.878	0.811	0.845	0.067	2.97
<b>5</b>	1.013	0.874	0.944	0.139	3.29
<b>6</b>	1.053	0.940	0.997	0.113	3.06
<b>7a</b>	1.113	— <sup>g</sup>	—	—	—
<b>7b</b>	1.019	0.902	0.961	0.117	3.34
<b>8a</b>	1.303	— <sup>g</sup>	—	—	—
<b>8b</b>	1.122	1.012	1.067	0.110	3.51
<b>8c</b>	1.116	1.020	1.068	0.096	3.65

<sup>a</sup>Glassy carbon electrode, Ag/AgCl, Pt, sweep rate: 0.1 V s<sup>-1</sup>. Potentials were shown as vs SHE. <sup>b</sup>Anodic peak potential. <sup>c</sup>Cathodic peak potential. <sup>d</sup> $E^{1/2} = (E_{pa} + E_{pc})/2$ . <sup>e</sup> $\Delta E = E_{pa} - E_{pc}$ . <sup>f</sup>The peak currents ( $i_{pa}$  and  $i_{pc}$ ) were measured from the respective baseline currents. <sup>g</sup>The current of the cathodic peak was too low to determine the potential value.

**FIGURE 2.** Cyclic voltammogram of nitroxides **1–3**. Nitroxides (2 mM) were dissolved in PBS (pH 7.4). Sweep rate: 0.1 V s<sup>-1</sup>.

reactants with **9**. The products were oxidized with hydrogen peroxide to obtain nitroxides **7b** and **8b**, respectively. Compound **17** was synthesized from the desulfurization of compound **16** and oxidized to afford the nitroxide **8c**. Compound **16** was refluxed in methanol in the presence of Raney-Ni to yield mainly compound **17** by partial desulfurization. When the same reaction was carried out in ethanol, it resulted in compound **3** by complete desulfurization.

**Cyclic Voltammetry.** The redox potentials of the nitroxides were determined by cyclic voltammetry in phosphate buffer saline (PBS, pH 7.4), using a glassy carbon electrode. Compounds **4** and **5** were measured in PBS containing 5% acetonitrile because of the solubility issues. Nevertheless, the redox potential of compound **1** did not vary under these two different conditions. Nitroxides undergo one-electron oxidation corresponding to the formation of *N*-oxoammonium cation. The redox potentials of this one-electron redox couple are listed in Table 1. The redox potentials of compounds **7a** and **8a** were not estimated because the cathodic peaks could not be measured. The peak separation,  $\Delta E = E_{pa} - E_{pc}$ , of compounds **1–4** was 58–70 mV, close to the theoretical Nernstian value of 59 mV. However, the intensities of the anodic and cathodic currents were not equal, indicating a slight loss of the kinetic reversibility. The redox

**TABLE 2.** Experimental Redox Potentials of Nitroxide/Deprotonated Hydroxylamine Redox Couple<sup>a</sup>

nitroxide	$E_{pa}^b$	$E_{pc}^c$	$E^{1/2d}$	$\Delta E^e$	$i_{pa}/i_{pc}^f$
<b>1</b>	0.524	−0.371	0.076	0.895	0.20
<b>2</b>	0.453	−0.401	0.026	0.854	0.20
<b>3</b>	0.226	−0.298	−0.036	0.524	2.12
<b>4</b>	0.244	−0.141	0.051	0.385	0.99
<b>5</b>	0.515	−0.364	0.076	0.879	0.09
<b>6</b>	0.644	−0.386	0.129	1.029	0.19
<b>7a</b>	0.613	−0.247	0.183	0.860	0.27
<b>7b</b>	0.585	−0.381	0.102	0.967	0.31
<b>8a</b>	0.653	−0.357	0.148	1.010	2.18
<b>8b</b>	0.694	−0.494	0.100	1.189	0.16
<b>8c</b>	0.416	−0.427	−0.006	0.844	0.22

<sup>a</sup>Glassy carbon electrode, Ag/AgCl, Pt, sweep rate: 0.1 V s<sup>-1</sup>. Potentials were shown as vs SHE. <sup>b</sup>Anodic peak potential. <sup>c</sup>Cathodic peak potential. <sup>d</sup> $E^{1/2} = (E_{pa} + E_{pc})/2$ . <sup>e</sup> $\Delta E = E_{pa} - E_{pc}$ . <sup>f</sup>The peak currents ( $i_{pa}$  and  $i_{pc}$ ) were measured from the respective baseline currents.

potentials ( $E^{1/2}$ ) of compounds **1–3** were found to decrease with the number of ethyl groups (Figure 2), suggesting the electron-donating substituents stabilize oxoammonium cations. Compounds **5**, **6**, **7b**, **8b**, and **8c** showed relatively larger  $\Delta E$  and higher peak current ratio, which correspond to the nitroxides with heteroatoms in the spiro ring. Moreover, the anodic and/or cathodic potentials of compounds **5**, **6**, **7a**, and **8a** were higher than those of the parent compound (**4**). These results indicate that substituents with heteroatoms (compounds **5–8**) destabilize oxoammonium cations because of the electron-withdrawing inductive effect.

A broad and irreversible wave was observed for one-electron reduction of nitroxide because of the hydroxylamine. The redox potentials for this redox-couple are listed in Table 2. The  $E^{1/2}$  values of compounds **1–3** decrease proportionally with the number of the ethyl group at the 2 and 6 positions, and the ethyl group had a greater impact on the anodic potential than the cathodic one. On the other hand, the  $E^{1/2}$  values of compounds **5**, **6**, **7a**, and **8a** were more positive than that of compound **4**. These results suggested that the electron-withdrawing groups at the 2 and 6 positions of the piperidine ring destabilize the nitroxides, while electron-donating substituents stabilize them. In addition, the comparison of compounds **7a** and **7b** (or **8a**, **8b**, and **8c**) showed that  $E^{1/2}$  values decreased when electron-withdrawing groups were replaced by the electron-donating groups methyl or ethyl. These results are also in agreement with the results of compounds **1–3**.

**Reactivity of 2,6-Substituted Piperidine Nitroxides with Ascorbate.** Nitroxides (25  $\mu$ M) were allowed to react with an excess of ascorbate (1 mM) and the rate of radical decay was monitored by using an X-band ESR spectrometer. The ESR signal decay rates of the nitroxides are shown in Figure 3. The nitroxide decay rate follows the order **1** > **2** > **3**, which is inversely proportional to the number of ethyl groups. Compound **3**, with four ethyl groups, was more resistant to the reduction than compound **2**, with two ethyl groups.

The reduction rates of compounds **5**, **6**, **7a**, and **8a** with ascorbate were found to be higher than that of their parent compound **4**. This can be explained by the presence of heteroatoms

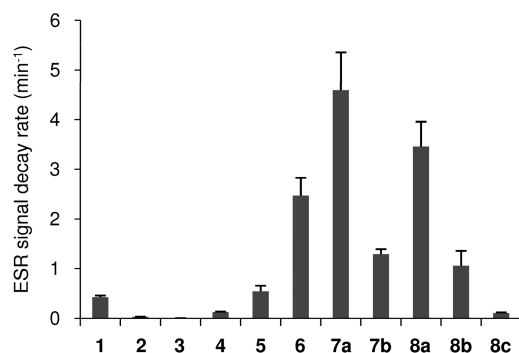


**FIGURE 3.** ESR signal decay rates of the reaction with ascorbate. Nitroxides (25  $\mu$ M) were allowed to react with an excess of ascorbate (1 mM) and the radical decay rate was monitored with an X-band ESR spectrometer. The values are the average of three experiments. Error bars shown are standard deviations.

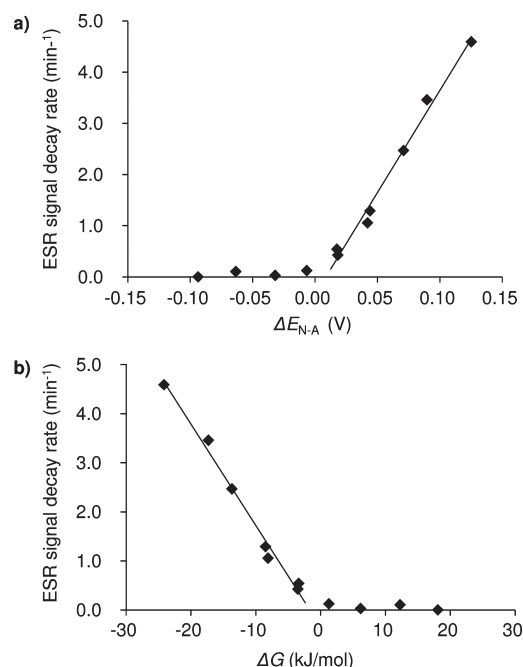


**FIGURE 4.** Relationship between the ESR signal decay rates and  $\Delta E_{N-A}$  (a) or  $\Delta G$  (b). (a)  $\Delta E_{N-A}$ : subtraction of the redox potential of ascorbate from that of nitroxides. (b)  $\Delta G$  was calculated from  $\Delta E_{N-A}$  with use of standard expression,  $\Delta G = -nF\Delta E_{N-A}$ , where  $n$  is the number of electrons per mole of product and  $F$  is the Faraday constant. The correlation coefficient when  $\Delta G$  was negative was 0.988.

in the spiro ring which act as an electron-withdrawing group and decrease the electron density around the N–O moiety, thereby favoring the reduction reaction. The trend of redox potentials for nitroxide reduction from electrochemical experiments is exactly the same as that of the nitroxide reduction rate by ascorbate, which supports our conclusions on the stabilization of nitroxides by substituents at the 2 and 6 positions.

**Relationship between the Redox Potential and the Reactivity with Ascorbate.** The relationship between the redox potential of the nitroxide and the reactivity with ascorbate

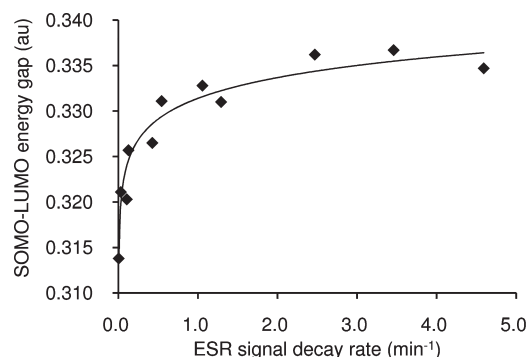


**FIGURE 5.** Plot of the SOMO-LUMO energy gap against ESR signal decay rate of nitroxides in ascorbic acid solution.

is shown in Figure 4a. The  $\Delta E_{N-A}$  value is the subtraction of the redox potential of the ascorbic acid (0.058 V vs standard hydrogen electrode, SHE)<sup>18</sup> from that of the nitroxide, which corresponds to the electromotive force. ESR signal decay rate increases with an increase in  $\Delta E_{N-A}$  and it approaches zero in the negative region of  $\Delta E_{N-A}$ . Substituents at the 4-position in a six-membered-ring nitroxide or at the 3-position in a five-membered-ring nitroxide were reported to influence the N–O reduction rate by ascorbate.<sup>12</sup> However, there is no report identifying the effect of substituents at 2 and 6 positions of the piperidine ring. Our results demonstrate a good correlation between the  $\Delta E_{N-A}$  value and the ESR signal decay rate of nitroxides differing in substituents proximate to the N–O moiety at 2 or 6 positions. To further understand the role of the substituents, the Gibbs free energy changes ( $\Delta G$ , calculated from the  $\Delta E_{N-A}$  by using the standard expression:  $\Delta G = -nF\Delta E_{N-A}$ ) were plotted against the ESR signal decay rate (Figure 4b). The ESR signal decay rate shows a good correlation with  $\Delta G$  in the negative  $\Delta G$  region ( $r^2 = 0.988$ ). The results indicate that reduction of the nitroxide by ascorbate occurred spontaneously when the  $\Delta G$  value was negative and that the reduction was not spontaneous when the  $\Delta G$  value was positive.

**Computational Studies.** The effect of substituents on the stability of nitroxide was further validated by computational methods. The nitroxides were modeled by using ab initio methods and various descriptors (SOMO and LUMO energies, geometry energy, and dipole moment) were calculated. These descriptors were analyzed to correlate with the stability of the nitroxides to reduction with ascorbate. The SOMO-LUMO energy gap of nitroxides showed a good correlation with their stability (Figure 5), the reduction rate of nitroxides increasing with an increase in the energy gap. This correlation can be explained by the hard and soft (Lewis) acids and bases theory—soft acids preferably react with soft bases and hard acids preferably react with hard bases.<sup>19</sup> The SOMO-LUMO energy gap of the radical corresponds to its absolute hardness and the higher the hardness, the higher is its reactivity with ascorbate. Hence, the nitroxides and ascorbate can be viewed as hard acids and hard bases, respectively. Moreover, the energy gap of nitroxide SOMO-ascorbate HOMO correlates with the ESR signal decay rate (Figure S15, Supporting Information). The SOMO energy levels of nitroxides were found to be higher

(18) Loach, P. A. In *Handbook of Biochemistry and Molecular Biology*, 3rd ed.; Fasman, G. D., Ed.; CRC Press: Cleveland, OH, 1976; p 123.

(19) Pearson, R. G. *J. Am. Chem. Soc.* **1985**, 107, 6801.



than the HOMO energy level of ascorbate. Ascorbate-mediated reduction is driven by the energy difference between nitroxide SOMO and ascorbate HOMO. Lower energy gaps facilitated the reaction and higher energy gaps retarded it. Electron-donating (ED) substituents raised the SOMO energy and made the radical nucleophilic, whereas electron-withdrawing (EW) substituents decreased the SOMO energy and increased the electrophilic nature (Table S2, Supporting Information). Hence ED groups decrease the reduction rate of nitroxides and EW groups increase the reduction rate. Nevertheless, it is to be pointed out that the reaction was found to correlate more closely with the SOMO-LUMO energy gap of nitroxides than that of nitroxide SOMO and ascorbate HOMO. This suggests that there is a possible involvement of nitroxide LUMO in the reduction reaction. However, the LUMO energy of nitroxides did not directly correlate with the reduction rate. Hence, it requires further investigation to understand the role of nitroxide LUMO in the reaction. To further investigate the role of steric factors in the stability of nitroxides, solvent accessible surface areas (ASA) of N–O atoms were calculated. ASA of N–O did not correlate with the stability to reduction, although the most stable compound **3** has the lowest ( $8.6 \text{ \AA}^2$ ) accessible area. The calculations suggest that although steric hindrance is a significant factor for nitroxides' stability, electronic factors play a dominant role in the stabilization.

## Conclusions

The redox potentials and the reduction rates of piperidine nitroxides were influenced by the electronic effect of substituents at 2 and 6 positions of the piperidine ring. A good correlation between the redox potential of the nitroxide and its reactivity toward ascorbate was demonstrated in this study. Molecular modeling studies indicated a good correlation between the SOMO-LUMO energy gap of nitroxides and the reduction rates. Stability and reactivity of a nitroxide go hand in hand with each other when such a compound is considered as a potential in vivo spin probe. Different stabilities and reactivities are desired for specific applications and hence it is important to optimize these properties for a given objective. Our electrochemical and molecular modeling studies consistently explained the effect of the substituent on the stability of nitroxides studied. Since there is a correlation between theoretically computed SOMO-LUMO energy gap and reduction rate, it is now possible to perform virtual screening of nitroxides, which rationally limits the need to synthesize all of the possible compounds, thereby increasing the chance of getting potential hits for better applications in vivo.

## Experimental Section

Reagents and solvents from commercial suppliers were used without further purification. Silica gel (100–200 mesh) was used for column chromatography. Nitroxide **1** was purchased from a commercial supplier and used as received. Nitroxides **3**–**6**, **7a**, **8a**, and **16** were synthesized as previously reported.<sup>17</sup>

**2,2-Dimethyl-9-thia-1-azaspiro[5.5]undecan-4-one (10).**  $\text{NH}_4\text{Cl}$  (4.8 g, 89.7 mmol) was added portionwise to a stirred solution of 1,2,2,6,6-pentamethylpiperidin-4-one **9** (2.25 g, 13.3 mmol) and tetrahydro-4*H*-thiopyrane-4-one (5.0 g, 43.1 mmol) in DMSO (30 mL) at room temperature, and the mixture was heated 14 h at 60 °C. The reaction mixture was diluted with  $\text{H}_2\text{O}$  (40 mL), followed by acidification with 7% aq HCl (10 mL), and then extracted with ether (3×) to remove a neutral fraction. The reaction

mixture was adjusted to pH 9 with 10% aq  $\text{K}_2\text{CO}_3$ , and extracted with AcOEt (4×). The AcOEt extract was washed with brine, dried over anhydrous sodium sulfate, and concentrated in vacuo. The residue was separated by column chromatography ( $\text{CHCl}_3$ ) to afford **10** as a brown oil (0.85 g, 30%). MS ( $\text{FAB}^+$ ) 214.24 ( $\text{M}^+ + 1$ );  $\nu_{\text{max}}/\text{cm}^{-1}$  1695 (C=O);  $^1\text{H}$  NMR (400 MHz;  $\text{CDCl}_3$ )  $\delta$  (ppm) 1.228 (s, 6H), 1.767 (ddd,  $J_1 = 12.2 \text{ Hz}$ ,  $J_2 = 3.2 \text{ Hz}$ , 2H), 1.907–1.950 (m, 2H), 2.229 (s, 2H), 2.281 (s, 2H), 2.394–2.430 (m, 2H), 3.003 (ddd, br, 2H);  $^{13}\text{C}$  NMR (75 MHz;  $\text{CDCl}_3$ )  $\delta$  (ppm) 24.0, 32.5, 40.9, 53.7, 54.8, 55.3, 56.2, 210.2. Anal. Calcd for  $\text{C}_{11}\text{H}_{19}\text{NOS}$ : C, 61.93; H, 8.98; N, 6.57. Found: C, 61.56; H, 8.93; N, 6.45.

**1,4-Dioxo-10-thia-14,14-dimethyl-13-azaspiro[4.1.5.3]penta-decane (11).** Compound **10** (426 mg, 2 mmol), PTSA (*p*-toluenesulfonic acid) (760 mg, 4 mmol), and ethylene glycol (0.22 mL, 4 mmol) in benzene (6 mL) were added to a round-bottomed flask equipped with a Dean–Stark apparatus to remove the water by azeotropic distillation. This solution was heated to 100 °C for 3 h. The resulting mixture was cooled to rt and adjusted to pH 10 with 10% aq  $\text{K}_2\text{CO}_3$ . This solution was extracted with  $\text{CHCl}_3$ , dried with  $\text{Na}_2\text{SO}_4$ , and evaporated in vacuo. The residue was purified by column chromatography with  $\text{CHCl}_3$  as the eluent to give **11** (346 mg, 67%). Mp 86.1–88.6 °C; MS ( $\text{FAB}^+$ ) 258.3 ( $\text{M}^+ + 1$ );  $\nu_{\text{max}}/\text{cm}^{-1}$  1056 (C=O);  $^1\text{H}$  NMR (400 MHz;  $\text{CDCl}_3$ )  $\delta$  (ppm) 1.202 (s, 6H), 1.507 (s, 2H), 1.554 (s, 2H), 1.809 (t, br, 2H), 1.99 (m, 2H), 2.44 (m, 2H), 2.928 (t, br, 2H), 3.934 (s, 4H);  $^{13}\text{C}$  NMR (75 MHz;  $\text{CDCl}_3$ )  $\delta$  (ppm) 24.0, 32.5, 40.7, 44.4, 45.9, 51.2, 52.0, 64.0, 109.0. Anal. Calcd for  $\text{C}_{13}\text{H}_{23}\text{NO}_2\text{S}$ : C, 60.66; H, 9.01; N, 5.44. Found: C, 60.26; H, 8.91; N, 5.34.

**7,7-Diethyl-9,9-dimethyl-1,4-dioxo-8-azaspiro[4.5]decane (12).** A slurry of freshly prepared Raney-Ni in methanol (3 mL) was added to a well-stirred solution of compound **11** (150 mg, 0.584 mmol) in methanol (5 mL) and the mixture was refluxed at 60 °C. After 1.5 h, the mixture was filtered through Celite and the filtrates concentrated in vacuo. The residue was separated by column chromatography to give the orange oil **12** (77 mg, 58%). MS ( $\text{FAB}^+$ ) 228.31 ( $\text{M}^+ + 1$ );  $\nu_{\text{max}}/\text{cm}^{-1}$  1091 (ketal);  $^1\text{H}$  NMR (400 MHz;  $\text{CDCl}_3$ )  $\delta$  (ppm) 0.797 (t,  $J = 7.4 \text{ Hz}$ , 6H), 1.202 (s, 6H), 1.329 (m, 2H), 1.502 (s, 2H), 1.551 (s, 2H), 1.703 (m, 2H), 3.931 (s, 4H);  $^{13}\text{C}$  NMR (75 MHz;  $\text{CDCl}_3$ )  $\delta$  (ppm) 7.9, 31.3, 32.3, 42.0, 45.9, 51.1, 56.0, 63.9, 109.4; HRMS ( $\text{FAB}^+$ ) calcd for  $\text{C}_{13}\text{H}_{26}\text{NO}_2$  [ $\text{M} + \text{H}$ ]<sup>+</sup> 228.1964, found 228.1999.

**2,2-Diethyl-6,6-dimethylpiperidin-4-one (13).** HCl aq (1.5 mL, 17.5–18.5%) was added dropwise to a well-stirred solution of compound **12** (77 mg, 0.339 mmol) in acetone (1 mL) and the mixture was stirred at rt for 6 h. The reaction mixture was diluted with  $\text{H}_2\text{O}$ , adjusted to pH 10 with  $\text{K}_2\text{CO}_3$  aq (10%), and extracted with  $\text{CHCl}_3$ . The extract was dried over  $\text{Na}_2\text{SO}_4$  and concentrated in vacuo. The residue was separated by column chromatography with hexane and ethyl acetate as the eluent to afford compound **13** (23 mg, 37%). MS ( $\text{FAB}^+$ ) 184.24 ( $\text{M}^+ + 1$ );  $\nu_{\text{max}}/\text{cm}^{-1}$  1708 (C=O);  $^1\text{H}$  NMR (400 MHz;  $\text{CDCl}_3$ )  $\delta$  (ppm) 0.836 (t,  $J = 7.6 \text{ Hz}$ , 6H), 1.224 (s, 6H), 1.384 (m, 2H), 1.511 (m, 2H), 2.228 (s, 2H), 2.266 (s, 2H);  $^{13}\text{C}$  NMR (75 MHz;  $\text{CDCl}_3$ )  $\delta$  (ppm) 8.0, 32.1, 32.2, 50.6, 54.5, 54.7, 59.9, 211.6. Anal. Calcd for  $\text{C}_{11}\text{H}_{21}\text{NO}$ : C, 72.08; H, 11.55; N, 7.64. Found: C, 71.86; H, 11.36; N, 7.54.

**2,2-Diethyl-6,6-dimethylpiperidin-4-one-1-oxyl (2).** Compound **13** (20 mg, 0.109 mmol) and  $\text{Na}_2\text{WO}_4 \cdot 2\text{H}_2\text{O}$  (18 mg, 0.055 mmol) were added to methanol (0.5 mL) and  $\text{H}_2\text{O}_2$  (30%, 0.2 mL) was slowly added to the solution with stirring for 24 h at rt. After being stirred, the solution was saturated with  $\text{K}_2\text{CO}_3$  and extracted with chloroform. The chloroform extracts were dried and evaporated. The residue was separated by column chromatography (hexane/AcOEt: 1/1) to afford yellow oil **2** (20 mg, 92%). MS ( $\text{FAB}^+$ ) 198.26 ( $\text{M}^+$ );  $\nu_{\text{max}}/\text{cm}^{-1}$  1713 (C=O). Anal. Calcd for  $\text{C}_{11}\text{H}_{20}\text{NO}_2$ : C, 66.63; H, 10.17; N, 7.06. Found: C, 66.58; H, 10.10; N, 6.98.  $A_N = 1.54 \text{ mT}$ .

**9-Acetyl-2,2-dimethyl-1,9-diazaspiro[5.5]undecan-4-one (14).**  $\text{NH}_4\text{Cl}$  (2.68 g, 50.0 mmol) was added portionwise to a stirred solution of **9** (1.69 g, 10.0 mmol) and 1-acetyl-4-piperidone (1.69 g, 12.0 mmol) in DMSO (8 mL) at room temperature, then the mixture was heated 4 h at 45 °C. The reaction mixture was diluted with  $\text{H}_2\text{O}$ , followed by acidification with 7% aq HCl, and then washed with ether (3 $\times$ ) to remove a neutral fraction. The reaction mixture was adjusted to pH 9 with 10% aq  $\text{K}_2\text{CO}_3$ , then extracted with  $\text{CHCl}_3$  (4 $\times$ ). The  $\text{CHCl}_3$  extract was washed with brine, dried over anhydrous sodium sulfate, and concentrated in vacuo. The residue was separated by column chromatography ( $\text{CHCl}_3/\text{MeOH}$ : 99/1) to afford compound **14** as a brown oil (238 mg, 10%). MS ( $\text{FAB}^+$ ) 239.2 ( $\text{M}^+ + 1$ );  $\nu_{\text{max}}/\text{cm}^{-1}$  1629 ( $-\text{N}-\text{CO}-$ ), 1708 ( $\text{C}=\text{O}$ );  $^1\text{H}$  NMR (400 MHz;  $\text{CDCl}_3$ )  $\delta$  (ppm) 1.188 (s, 3H), 1.222 (s, 3H), 1.496–1.691 (m, 4H), 2.048 (s, 3H), 2.271 (s, 2H), 2.294 (s, 2H), 3.343–3.781 (m, 4H);  $^{13}\text{C}$  NMR (75 MHz;  $\text{CDCl}_3$ )  $\delta$  (ppm) 21.5, 37.6, 40.0, 42.6, 52.4, 55.9, 168.9, 208.7; HRMS ( $\text{ESI}^+$ ) calcd for  $\text{C}_{13}\text{H}_{23}\text{N}_2\text{O}_2$  [ $\text{M} + \text{H}$ ] $^+$  239.1760, found 239.1741.

**9-Acetyl-2,2-dimethyl-1,9-diazaspiro[5.5]undecan-4-one-9-oxyl (7b).** Compound **14** (0.28 g, 1.17 mmol) was oxidized according to the method described for compound **2**. Yield 40% (0.12 g); mp 162–163 °C; MS ( $\text{FAB}^+$ ) 337.3 ( $\text{M}^+ + 1$ );  $\nu_{\text{max}}/\text{cm}^{-1}$  1720 ( $\text{C}=\text{O}$ ), 1637 ( $-\text{N}-\text{CO}-\text{CH}_3$ ); HRMS ( $\text{ESI}^+$ ) found 276.1467, calcd for  $\text{C}_{13}\text{H}_{21}\text{N}_2\text{O}_3$  ([ $\text{M} + \text{Na}$ ] $^+$ ) 276.1450;  $A_N = 1.58$  mT.

**2,2-Dimethyl-9-thia-4,9,9-trioxo-1-azaspiro[5.5]undecane (15).** Tetrahydro-4H-thiopyran-4-one 1,1-dioxide (2.0 g, 13.5 mmol) was used in place of tetrahydro-4H-thiopyran-4-one according to the method described for compound **10**. Yield 13% (145 mg); mp 182.9 °C (hexane–AcOEt); MS ( $\text{FAB}^+$ ) 246.1 ( $\text{M}^+ + 1$ );  $\nu_{\text{max}}/\text{cm}^{-1}$  1698 ( $\text{C}=\text{O}$ ), 1291 ( $\text{SO}_2$ );  $^1\text{H}$  NMR (300 MHz;  $\text{CDCl}_3$ )  $\delta$  (ppm) 1.253 (s, 6H), 2.044–2.229 (m, 4H), 2.282 (s, 2H), 2.326 (s, 2H), 2.811–2.872 (m, 2H), 3.491 (ddd,  $J_1 = 13.2$  Hz,  $J_2 = 3.8$  Hz, 2H);  $^{13}\text{C}$  NMR (75 MHz;  $\text{CDCl}_3$ )  $\delta$  (ppm) 31.5, 36.9, 47.4, 53.1, 54.9, 55.6, 56.0, 208.6. Anal. Calcd for  $\text{C}_{11}\text{H}_{19}\text{NO}_3$ : C, 53.85; H, 7.81; N, 5.71. Found: C, 53.84; H, 7.86; N, 5.75.

**2,2-Dimethyl-9-thia-4,9,9-trioxo-1-azaspiro[5.5]undecane-9-oxyl (8b).** Compound **15** (145 mg, 0.59 mmol) was oxidized according to the method described for compound **2**. The crude product was recrystallized from AcOEt to give **8b**. Yield 153 mg (99%); mp 157.5–160.8 °C; MS ( $\text{FAB}^+$ ) 261.2 ( $\text{M}^+ + 1$ );  $\nu_{\text{max}}/\text{cm}^{-1}$  1714 ( $\text{C}=\text{O}$ ), 1296 ( $\text{SO}_2$ ). Anal. Calcd for  $\text{C}_{11}\text{H}_{18}\text{NO}_4$ : C, 50.75; H, 6.97; N, 5.38. Found: C, 50.85; H, 7.00; N, 5.26.  $A_N = 1.54$  mT.

**2,2-Diethyl-9-thia-1-azaspiro[5.5]undecan-4-one (17).** A slurry of freshly prepared Raney-Ni in methanol (6 mL) was added to a well-stirred solution of compound **16**<sup>17</sup> (1.1 g, 4.24 mmol) in methanol (20 mL) and the mixture was refluxed at 75 °C. After 3 h, the mixture was filtered through Celite and the filtrates were concentrated in vacuo. The residue was separated by column chromatography (hexane/AcOEt = 1/1) to give the light yellow oil **17** (284 mg, 32%). MS ( $\text{FAB}^+$ ) 242.3 ( $\text{M}^+ + 1$ );  $\nu_{\text{max}}/\text{cm}^{-1}$  1708 ( $\text{C}=\text{O}$ );  $^1\text{H}$  NMR (300 MHz;  $\text{CDCl}_3$ )  $\delta$  (ppm) 0.853 (t,  $J = 7.2$  Hz, 6H), 1.430 (q,  $J = 7.2$  Hz, 2H), 1.442 (q,  $J = 7.5$  Hz, 2H), 1.840 (ddd,  $J_1 = 7.9$  Hz,  $J_2 = 3.5$  Hz, 4H), 2.265 (s, 2H), 2.267 (s, 2H), 2.439–2.517 (m, 2H), 2.867–2.954 (m, 2H);  $^{13}\text{C}$  NMR (75 MHz;  $\text{CDCl}_3$ )  $\delta$  (ppm) 8.1, 24.3, 33.0, 41.7, 50.4, 52.6, 54.9, 59.3, 210.7. Anal. Calcd for  $\text{C}_{13}\text{H}_{23}\text{NOS}$ : C, 64.68; H, 9.60; N, 5.80. Found: C, 64.66; H, 9.70; N, 5.76.

**2,2-Diethyl-9-thia-4,9,9-trioxo-1-azaspiro[5.5]undecane-9-oxyl (8c).** Compound **17** (284 mg, 1.18 mmol) was oxidized according to the method described for compound **2**. The crude

product was recrystallized from hexane/AcOEt to give orange crystals of **8c**. Yield 260 mg (77%); mp 116.1–121.2 °C; MS ( $\text{FAB}^+$ ) 289.3 ( $\text{M}^+ + 1$ );  $\nu_{\text{max}}/\text{cm}^{-1}$  1715 ( $\text{C}=\text{O}$ ), 1292 ( $\text{SO}_2$ ). Anal. Calcd for  $\text{C}_{13}\text{H}_{22}\text{NO}_4\text{S}$ : C, 54.14; H, 7.69; N, 4.86. Found: C, 54.17; H, 7.66; N, 4.80.  $A_N = 1.49$  mT.

**Cyclic Voltammetry.** The electrochemical experiments were conducted in a sealed, three-electrode glass cell. A platinum wire and Ag/AgCl electrode were used as counter and reference electrodes, respectively. A glassy carbon electrode with a disk diameter of 1 mm was used as the working electrode. The working electrode was polished with polishing alumina suspension and a polishing cloth, and rinsed with deionized distilled water. All electrochemical measurements were performed in PBS (pH 7.4). Before collecting cyclic voltammograms, the solution was purged with argon gas for 10 min to minimize the effect of molecular oxygen and the inert atmosphere was maintained by a continuous argon flow over the solution during the experiment. The cyclic voltammograms were collected at ambient temperature at potential sweep rates of 0.1 V s $^{-1}$ .

**Rate Constant of Reaction with Ascorbate.** A solution of nitroxides (50  $\mu\text{M}$ ) in PBS (pH 7.4) containing 100  $\mu\text{M}$  diethylenetriaminepentaacetic acid (DTPA) was prepared. Sodium ascorbate solution (2 mM) was prepared in PBS (pH 7.4) with 100  $\mu\text{M}$  DTPA and was mixed in an equal amount of nitroxide solution. The resulting mixture of nitroxides (25  $\mu\text{M}$ ) and ascorbate (1 mM) was immediately taken up into a quartz capillary and then introduced into an ESR tube and transferred into the cavity of an ESR spectrometer. The ESR spectra were recorded at room temperature as a function of time. Each experiment was repeated three times. The loss of signal intensity of the low magnetic field ESR signal was measured and fitted to exponential decay to compute the rate constants of each nitroxide.

**ESR Spectra Measurement.** ESR experimental conditions were the following: frequency, 9.4 GHz; power, 10 mW; magnetic field, 334 mT; modulation amplitude, one-third of the line width of each nitroxides; and time constant, 0.03 s.

**Molecular Modeling.** The General Atomic and Molecular Electronic Structure System (GAMESS)<sup>20</sup> in conjunction with the Ghemical<sup>21</sup> program was used for geometry optimization and other calculations of all nitroxides. The Ghemical program was used to generate input structures for GAMESS. Input structures were energy minimized with AMBER force field<sup>22</sup> prior to ab initio calculations. SCF wave function, restricted open shell Hartree–Fock (ROHF)<sup>23</sup> was used with Pople's STO-nG Gaussian minimal basis set<sup>24</sup> for calculating equilibrium geometry. Orbital symmetry was not forced during the calculation. All the calculations were done until the SCF converged. Energy values of SOMO, LUMO, total geometry energy, solvent-accessible surface area (with 1.4 Å radius probe), and dipole moment were calculated for the equilibrium structure.

**Acknowledgment.** This study was partially supported by the Development of Systems and Technology for Advanced Measurement and Analysis of the Japan Science and Technology Agency, and a Grant-in-Aid for Young Scientists from the Japan Society for the Promotion of Science.

**Supporting Information Available:**  $^1\text{H}$  and  $^{13}\text{C}$  NMR spectra of nonradical intermediates in Scheme 1, ESR parameters, calculated descriptors, supplemental figure, STO-3G/ROHF optimized coordinates of nitroxides, and corresponding total energy. This material is available free of charge via the Internet at <http://pubs.acs.org>.

(20) Michael, W. S.; Kim, K. B.; Jerry, A. B.; Steven, T. E.; Mark, S. G.; Jan, H. J.; Shiro, K.; Nikita, M.; Kiet, A. N.; Shujun, S.; Theresa, L. W.; Michel, D.; John, A. M., Jr. *J. Comput. Chem.* **1993**, *14*, 1347.

(21) Tommi, H.; Mikael, P. *J. Comput. Chem.* **2001**, *22*, 1229.

(22) Wang, J.; Wolf, R. M.; Caldwell, J. W.; Kollman, P. A.; Case, D. A. *J. Comput. Chem.* **2004**, *25*, 1157.

(23) Guest, M. F.; Saunders, V. R. *Mol. Phys.* **1974**, *28*, 819.

(24) Davidson, E. R.; Feller, D. *Chem. Rev.* **1986**, *86*, 681.